Large $N \times N$ Waveguide Grating Routers

P. Bernasconi, *Member, OSA*, C. Doerr, *Member, IEEE*, C. Dragone, *Fellow, IEEE*, M. Cappuzzo, E. Laskowski, and A. Paunescu

***Abstract*—We show how the grating diffraction properties of a $N \times N$ waveguide grating router (WGR) can limit the size of N when the device operates with a unique set of N wavelengths as a strict-sense nonblocking $N \times N$ cross connect. We motivate why, for large N, the N optical channels should be chosen equally spaced in wavelength and not in frequency. Two different approaches to increase N are presented. We report on results obtained in a 40×40 and a 80×80 WGR.**

***Index Terms*—Crosstalk, optical filters, waveguide gratings, wavelength-division multiplexing (WDM).**

I. Introduction

LARGE $N \times N$ waveguide grating routers (WGR's) represent an excellent solution for large optical cross connects: They are fully passive elements and they can provide strictly nonblocking connections for a set of N optical channels [1]–[5].

However, due to the intrinsic diffraction characteristics of the grating, restrictions apply to the size of N. As we shall demonstrate, this generally happens when N approaches the diffraction order m at which the grating operates. Additional and even more severe limitations arise if the WGR is designed to cross connect channels which are equally spaced in frequency. Different approaches have been undertaken to improve the capacity of the WGR's but often at the cost of additional losses [6] or by sacrificing the characteristic periodicity of these structure [4].

In the following, the maximization of N is discussed for channels equally spaced either in frequency or in wavelength. For the latter case, we show how N can be further increased by appropriate arrangements in the design of the device and/or by slightly correcting the channels wavelengths. The results are successfully implemented in a 40×40 WGR operating with a single set of 40 wavelengths equally spaced by 0.4 nm.

II. Grating Diffraction Properties

The WGR consists of two $N \times M$ star couplers connected by M waveguides of unequal length, [1] as shown in Fig. 1. The functionality of a diffraction grating is obtained by letting the length of the M waveguides increase linearly. With a proper design, when every input port carries the same set of N optical channels, each output port receives N different channels each coming from a different input. This provides the $N \times N$ strict-sense nonblocking cross connect [1], [7].

The size of N is primarily given by the diffraction properties of the grating and secondarily by the spectral dispersion of the material refractive indexes. By first neglecting the latter correction terms, for small diffraction angles[1] the angular aperture between each two diffracted signals of input waves equally spaced in *wavelength* is a constant. This follows from the well-known relation

$$a(\sin \vartheta_\lambda^{\text{in}} - \sin \vartheta_\lambda^{\text{out}}) = m\lambda \tag{1}$$

where

- a grating period;
- m integer;
- $\vartheta_\lambda^{\text{in/out}}$ incident and the diffracted angles for the wavelength λ in the material and/or waveguide.

For small angles and for two neighboring wavelengths λ and $\lambda'(\equiv \lambda + \Delta\lambda)$incident under the same angle, (1) simplifies into

$$\Delta\vartheta^{\text{out}} \equiv \vartheta_{\lambda'}^{\text{out}} - \vartheta_\lambda^{\text{out}} \approx \frac{m}{a}(\lambda' - \lambda) = \frac{m}{a}\Delta\lambda \tag{2}$$

where $\Delta\vartheta^{\text{out}}$ is independent of both the wavelength and the incident angle ϑ^{in}. The latter conclusion is not valid when (1) and (2) are expressed in term of frequency with $\nu' \equiv \nu + \Delta\nu$. Thus for a given grating order m, $\Delta\vartheta^{\text{out}}$ is proportional to $\Delta\lambda$.

The angles of incidence can be chosen so that the different sets of output angles belonging to each ϑ^{in} overlap, although mutually shifted by $\Delta\vartheta^{\text{out}}$. So, for N evenly spaced wavelengths incident under each of the N input angles will cover a set of only $2N$ output angles, as shown in Fig. 2(a) and (b). However, the overlapping among wavelengths coming from different input angles might not be perfect if the effects of the wavelength dispersion of the refractive indexes are included. We define the wavelengths as

$$\lambda_j \equiv \lambda_0 - j\Delta\lambda \tag{3}$$

with $j = 0, \pm 1, \pm 2, \ldots, \pm N/2$. Staying in the same diffraction order m, the output angular mismatch experienced by λ_j incident under the input angle ϑ_i (with respect to case where the central incident angle $\vartheta_{i=0}$ is used) is of the kind

$$\begin{aligned}\delta\vartheta_{j,i}^{\text{out}} = {} & \frac{m}{a}\frac{\lambda_0}{n_w(\lambda_0)} \\ & \cdot\left\{\frac{1}{n_w(\lambda_0)}\left[\frac{n_w(\lambda_j)-n_w(\lambda_0)}{n_f(\lambda_j)} - \frac{n_w(\lambda_i)-n_w(\lambda_0)}{n_f(\lambda_i)} \right.\right. \\ & \left. - \frac{n_w(\lambda_{j-i})-n_w(\lambda_0)}{n_f(\lambda_{j-i})}\right] \\ & \left. + \frac{\Delta\lambda}{\lambda_0}\left[\frac{j}{n_f(\lambda_j)} - \frac{i}{n_f(\lambda_i)} - \frac{j-i}{n_f(\lambda_{j-i})}\right]\right\}. \end{aligned} \tag{4}$$

Manuscript received December 3, 1999; revised March 23, 2000.

The authors are with the Bell Laboratories, Lucent Technologies, Holmdel, NJ 07733 USA.

Publisher Item Identifier S 0733-8724(00)05757-1.

[1]Due to the analogy between WGR's and bulk gratings, we use interchangeably the terms input (output) ports of the WGR and incident (diffracted) angles at the grating.

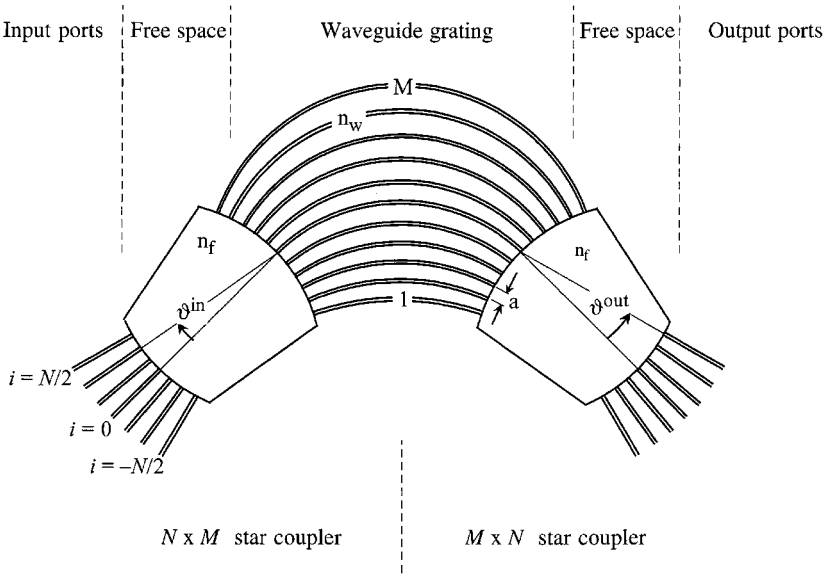

Fig. 1. Scheme of a $N \times N$ WGR where the free spaces of the two $N \times M$ star couplers are connected by M grating arms. The refractive indexes n_f and n_w refer to the light propagating in the free space and in the waveguide, respectively.

Equation (4) vanishes when the dispersion of the refractive indexes is neglected. In (4), n_w and n_f refer to the refractive indexes of light propagating in the waveguides and in the free space, respectively, inside a WGR (see Fig. 1).

On the other hand, for optical channels equally spaced in frequency ($\nu_j \equiv \nu_0 + j\Delta\nu$), (4) reads as

$$\delta\vartheta_{j,i}^{\text{out}} = \frac{m}{a}\frac{c}{\nu_0 n_w(\nu_0)} \cdot \left\{ \frac{1}{n_f(\nu_j)}\left[n_w(\nu_j) - n_w(\nu_0)\frac{\nu_0}{\nu_j}\right] - \frac{1}{n_f(\nu_i)}\left[n_w(\nu_i) - n_w(\nu_0)\frac{\nu_0}{\nu_i}\right] - \frac{1}{n_f(\nu_{j-i})}\left[n_w(\nu_{j-i}) - n_w(\nu_0)\frac{\nu_0}{\nu_{j-i}}\right]\right\}. \tag{5}$$

Here, $\delta\vartheta_{\text{out}}^{j,i}$ does not vanish even by neglecting the dispersion of the refractive indexes. Further, (5) is explicitly frequency dependent which deteriorates the overlapping when frequency and input angle deviate from the central frequency ν_o and from the central input angle ϑ_0, respectively. Nevertheless, the deviation is small as long as

$$\frac{\delta\vartheta_{\text{out}}^{j,i}}{\Delta\vartheta} = \frac{1/\nu_i - 1/\nu_j}{1/\nu_{(j-i\pm1)} - 1/\nu_0} \ll 1. \tag{6}$$

A bad overlapping leads to a deterioration of the device characteristics. So, in $N \times N$ WGR's the optical channels have to be equally spaced in wavelength if the optimum performance in terms of losses and crosstalk is preferred. However, this fundamental requirement stays latent in devices designed for channels equally spaced in frequency as long as the covered frequency span is small enough. How small is "small enough" shall be quantified in the following by taking (6) as a starting point.

III. The Wrap-Around Limitations

The discussion presented in the previous section assumes the WGR to operate with a fixed diffraction order m. Additional restrictions arise when the mapping input-output ports is achieved by using different diffraction orders. This situation occurs when the $N \times N$ WGR has to operate with a unique set of N wavelengths or frequencies for all input ports. As illustrated in Fig. 2(b) and (c), by shifting the input port the diffracted channels are distributed over a shifted angular sector which partially falls outside the sector covered by the N output ports. The $N \times N$ connectivity is lost. To obviate this inconvenient, the next higher and next lower diffraction orders are used to setup the so called periodic grating response or wrap-around. By an appropriate choice of the grating period a, as soon as one channel falls out on one side of the angular sector covered by the output ports, the next diffraction order moves in from the other side replacing the "lost" channel with its copy in the next diffraction order.

However, the resort to different diffraction order introduces additional misalignments. The origin resides in (2) which clearly shows that the angular aperture between two neighboring channels entering the same input port depends on the diffraction order m. Therefore, by using the same input ports the overlapping among the diffracted channels belonging to different diffraction order is lost.

For channels equally spaced in *wavelength*, although $\Delta\vartheta^{\text{out}}$ is still constant inside each diffraction order, the misalignment expressed by (4) has to be corrected when $|j-i| > N/2$ into

$$\delta\vartheta_{j,i}^{\text{out}} = \frac{m\lambda_0}{a n_w(\lambda_0)} \cdot \left\{ \frac{1}{n_w(\lambda_0)}\left[\frac{n_w(\lambda_j) - n_w(\lambda_0)}{n_f(\lambda_j)} - \frac{n_w(\lambda_i) - n_w(\lambda_0)}{n_f(\lambda_i)} - \frac{n_w(\lambda_{j-i\pm N}) - n_w(\lambda_0)}{n_f(\lambda_{j-i\pm N})}\right]\right.$$

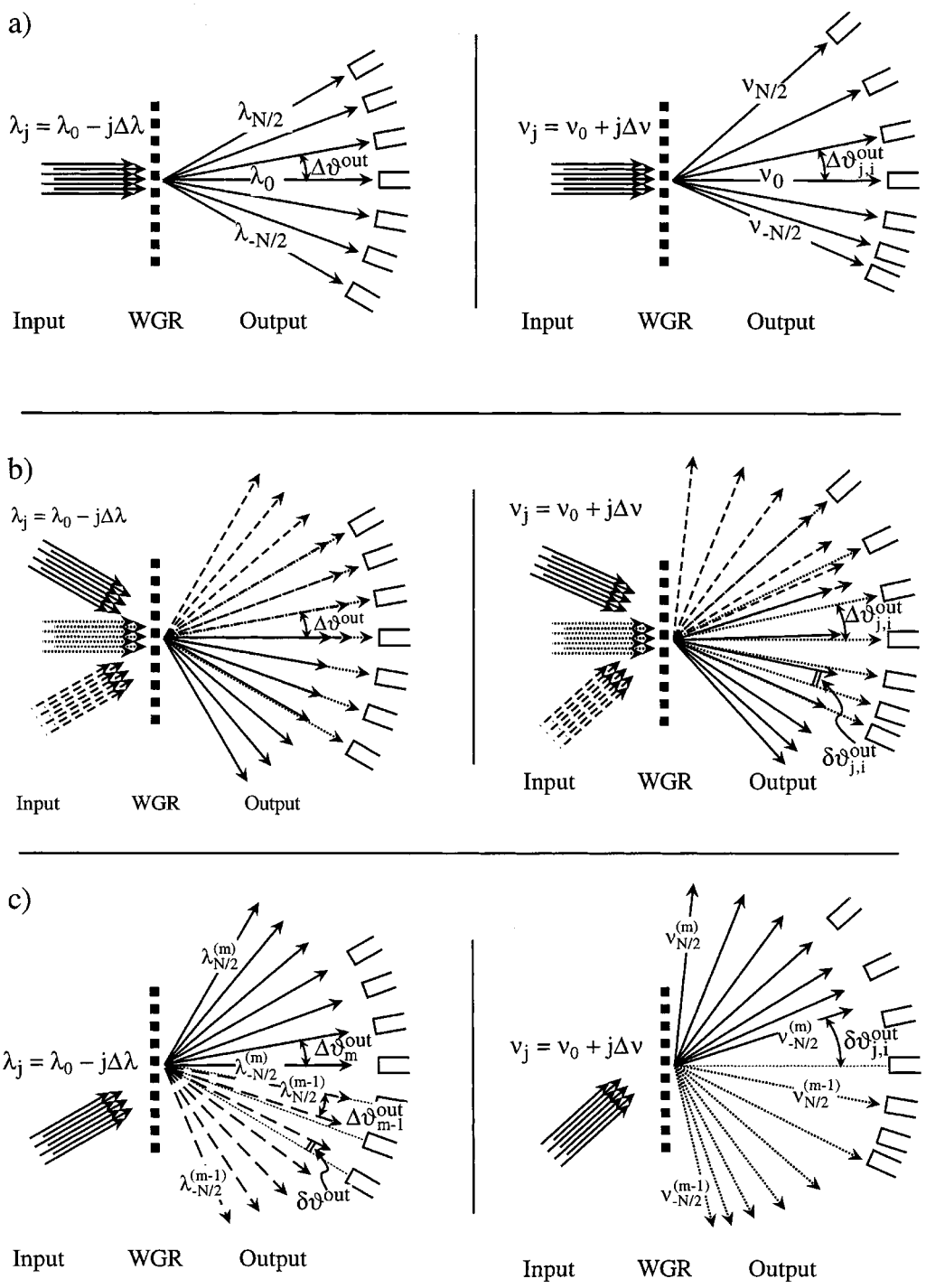

Fig. 2. Diffraction at a WGR for channels equally spaced in wavelength (left) and in frequency (right). (a) Diffraction with a fixed input port and fixed diffraction order m. (b) Diffraction with different input ports and fixed diffraction order m. (c) Diffraction with a fixed input port and two different diffraction orders m and $m-1$.

$$+\frac{\Delta\lambda}{\lambda_0}\left[\frac{j}{n_f(\lambda_j)}-\frac{i}{n_f(\lambda_i)}-\frac{j-i\pm N}{n_f(\lambda_{j-i\pm N})}\right]\Bigg\}\pm\frac{\lambda_0-j\Delta\lambda}{a\cdot n_f(\lambda_j)} \tag{7}$$

which, in a first approximation, can be simplified to

$$\delta\vartheta^{\text{out}}_{j,i}\approx\mp\frac{j\Delta\lambda}{a\cdot n_f(\lambda_j)}. \tag{8}$$

The misalignment increases linearly with the distance between the central wavelength λ_0 and the wavelength λ_j diffracted in the next higher (sign $-$) or in the next lower (sign $+$) diffraction order. Notice that, by neglecting the wavelength dispersion of the refractive indexes, the misalignment for a specific channel does not depend on the input port.

Thus, half of the angular separation between two output ports $(\Delta\vartheta^{\text{out}}/2)$ combined with the maximum value of $\delta\vartheta^{\text{out}}$ define an upper limit for the wavelength span $N\cdot\Delta\lambda$ and, for

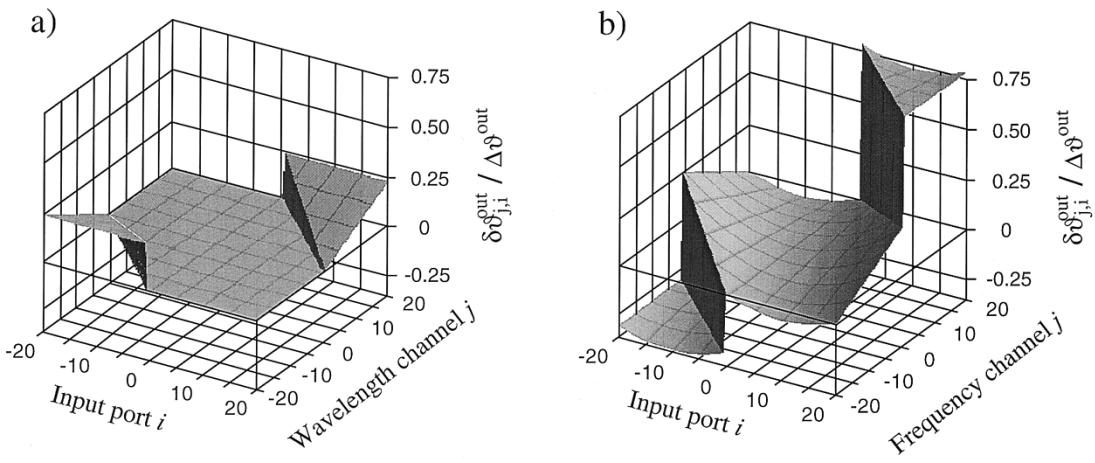

Fig. 3. Calculated relative angular deviation $\delta\vartheta^{\rm out}/\Delta\vartheta^{\rm out}$ as a function of the input port i and the optical channel j for channels equally spaced in (a) wavelength or (b) frequency in a 41×41 WGR. The wavelength channels are defined as $\lambda_j = \lambda_0 - j\,\Delta\lambda$ where $\lambda_0 = 1555$ nm and $\Delta\lambda = 0.4$ nm. The frequency channels are defined as $\nu_j = \nu_0 + j\Delta\nu$ where $\nu_0 = c/\lambda_0$ and $\Delta\nu = 50$ GHz.

a given channel spacing $\Delta\lambda$, how many channels can be efficiently cross connected. According to (8), the maximum deviation $\delta\vartheta^{\rm out}_{\rm max}$ occurs with the longest or the shortest wavelength, i.e., when $j = \pm N/2$ so that the previous condition

$$\delta\vartheta^{\rm out}_{\rm max} \ll \Delta\vartheta^{\rm out}/2 \tag{9}$$

can be expressed as

$$\frac{\delta\vartheta^{\rm out}_{\rm max}}{\Delta\vartheta^{\rm out}} = N^2\frac{\Delta\lambda}{\lambda_0}\frac{n^g_w}{n_w(\lambda_0)} = \frac{N}{m} \ll 1 \tag{10}$$

where n^g_w is the group index in the waveguides. As already mentioned, (10) gives only an upper limit for the usable wavelength span, because in a real device the tolerated misalignment is set by design and performance parameters such as the width of the output ports, the affordable additional losses, and crosstalk level.

An equivalent approach can be followed for channels equally spaced in *frequency* although the analysis of this case presents a higher degree of complexity due to the fact that, as already mentioned, $\Delta\vartheta^{\rm out}$ is not a constant for a given diffraction order m and due to the fact that $\delta\vartheta^{\rm out}_{j,i}$ is an explicit function of the frequency. Instead of presenting the abstruse equation for $\delta\vartheta^{\rm out}_{j,i}$, the consequences of channel equally spaced in frequency shall be illustrated graphically in the following section.

IV. Wavelength Versus Frequency: An Example

As a corollary to the equations, we motivate why large $N\times N$ WGR's operating with a single set of N optical channels should be designed for equally spaced wavelengths and not frequencies by evaluating in the two cases $\delta\vartheta^{\rm out}_{j,i}/\Delta\vartheta^{\rm out}$ for $N = 41$. The relative deviation is calculated as a function of both the input port i and the wavelength or frequency channel j. The channel spacing is $\Delta\lambda = 0.4$ nm or $\Delta\nu = 50$ GHz, respectively. The refractive indexes correspond to devices fabricated in silica where the spectral dispersion can be safely neglected over the spectral range of interest centered at $\lambda_0 = 1555$ nm.

The difference between the two curves shown in Fig. 3 is substantial: The WGR designed for channels equally spaced in wavelength performs better. Both the maximum deviation $\delta\vartheta^{\rm out}_{\rm max}$ as well as the misalignment at each single (j, i)-combination are remarkably smaller than in the case for channels equally spaced in frequency.

In Fig. 3(a), for channels equally spaced in wavelength, (4) defines the flat central region where the almost vanishing deviation is given by the negligible wavelength dispersion of the refractive indexes in silicon. The resort to different diffraction orders is the origin of the "wings" characterized by the linear increase for increasing deviation from λ_0 as described by (8). It is worth noting that the deviation at the "wings" has always the same sign. We will be right back to this peculiarity.

In Fig. 3(b), for channels equally spaced in frequency, (5) defines a curved central region in which the worst case is already even worse than $\delta\vartheta^{\rm out}_{\rm max}$ calculated for evenly spaced wavelengths. Similarly to Fig. 3(a), the use of different diffraction orders produces "wings" but, in this case, with much higher amplitudes and with opposite sign. We finally mention that for the same $\delta\vartheta^{\rm out}_{\rm max}$ obtained in a 41×41 WGR with channel equally spaced in frequency, for evenly spaced wavelengths the WGR could be as large as 71×71.

Once again, we remind that these curves do not take into account the restrictions imposed by design and performance parameters such as the width of the output ports, the affordable additional losses, and tolerated crosstalk level.

V. Improvements

In Fig. 3(a) the curve always assumes positive values and the deviation ranges from ~ 0 in the central region to $\vartheta^{\rm out}_{\rm max} \sim 0.25$ for the shortest and the longest wavelengths at the "wings". This peculiar property allows us to halve the value of $\delta\vartheta^{\rm out}_{\rm max}$ by shifting the position of the output ports by half of this angle. The result is shown in Fig. 4(a). This procedure will degrade the angular deviation in the flat region of the curve but it will allow either to halve $\delta\vartheta^{\rm out}_{\rm max}$ or to double the number of channels N by keeping $\delta\vartheta^{\rm out}_{\rm max}$ unchanged.

Similar improvements can also be obtained by a fine tuning of the N equally spaced wavelengths instead of shifting the output ports. With a parabolic detuning of the equally spaced wavelengths, as the one shown in Fig. 5 around the central wavelength, it is possible to minimize $\delta\vartheta^{\rm out}_{\rm max}$ to about half of the orig-

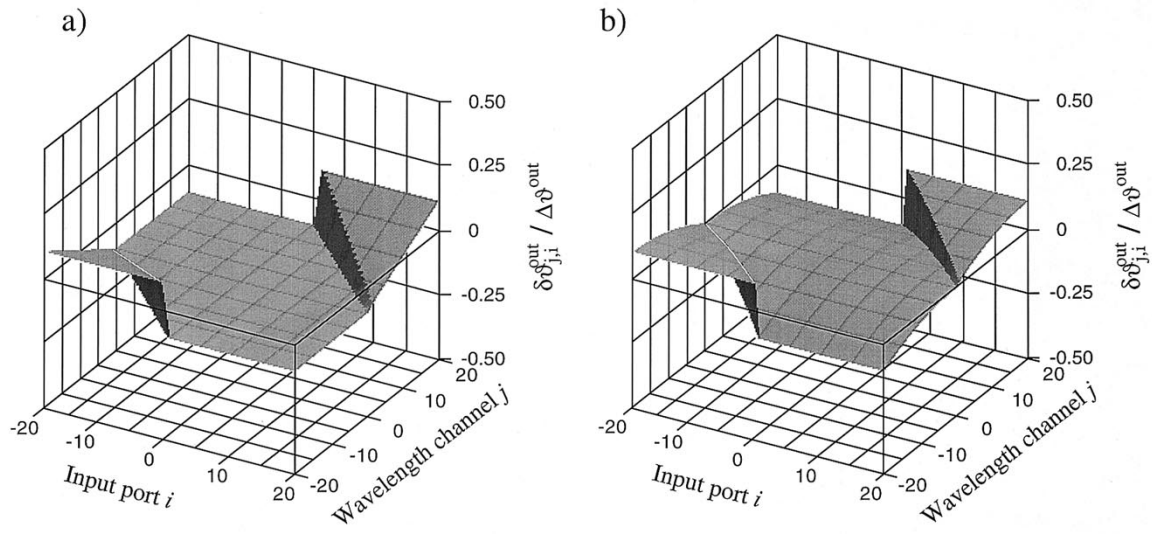

Fig. 4. Calculated relative angular deviation $\delta\vartheta^{\text{out}}/\Delta\vartheta^{\text{out}}$ as a function of the input port i and the optical channel j in a 41×41 WGR. (a) For channels equally spaced in wavelength and shifted output ports. (b) For parabolically detuned wavelengths (see also Fig. 5). Details in the text.

inal value. For comparison the relative deviation $\delta\vartheta^{\text{out}}_{j,i}/\Delta\vartheta^{\text{out}}$ is plotted in Fig. 4(b) where it can be noticed that the global performance in this case is slightly better.

These two approaches can be also implemented for channels equally spaced in frequency but the improvements that can be achieved are insignificant.

VI. Experimental Results

A 40×40WGR has been designed for channels with wavelengths equally spaced by $\Delta\lambda = 0.4$ nm. To reduce $\delta\vartheta^{\text{out}}_{\max}$ the position of the output ports has been uniformly shifted by half of this angle, as explained in Section V. The device operates with a diffraction order $m = 95$ which, with $N = 40$, approximately fulfills (10). However, as already mentioned, the stringent limits for the deviation $\delta\vartheta^{\text{out}}_{j,i}$ are given by the angular aperture covered by one output port which is of course smaller than $\Delta\vartheta$. In our case, we calculate that $\delta\vartheta^{\text{out}}_{j,i}$ deviates from the axis of the output ports by less than one fifth of the total angular aperture covered by a single output port.

Such small misalignment can be revealed by the calculated transmission spectrum of the device. The peaks can be shown to be not perfectly spaced by 0.4 nm but to slightly drift from the exact position. The worst channel mismatch is less than 10% of the channel spacing and from such misalignment an additional loss of less than 1.5 dB is expected at the exact wavelength.

The measured transmission spectrum is shown in Fig. 6(a) and (b) where each curve represents the transmission spectrum obtained at the 40 different output ports when a white source illuminates one input port. The positions of the peaks agree very well with the calculations although globally shifted by 0.8 nm toward shorter wavelengths. The insertion losses measured at the peaks range from 4 and 6 dB while the additional loss due to $\delta\vartheta^{\text{out}}_{j,i}$ is less than 1.5 dB in the worst case. Thus, this WGR can operate as a 40×40 cross connect with one set of 40 wavelengths.

For completeness, we mention that the adjacent crosstalk level is about -25 dB while the average crosstalk level is 5 dB

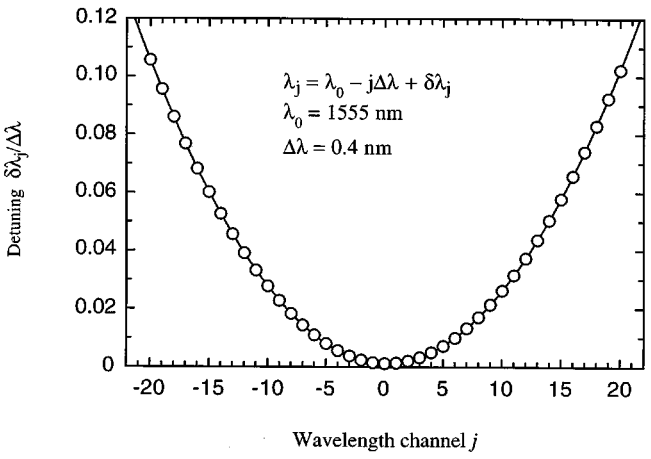

Fig. 5. Calculated detuning from the exact equally spaced wavelengths which minimizes the relative maximum angular deviation $\delta\vartheta^{\text{out}}_{\max}/\Delta\vartheta^{\text{out}}$ in a 41×41 WGR. $\lambda_j = \lambda_0 - j\Delta\lambda + \delta\lambda_j$ with $\lambda_0 = 1555$ nm and $\Delta\lambda = 0.4$ nm.

lower. These values shall be improved by a more precise design of the device and a more accurate fabrication process.

To push N even further, an 80×80 WGR has been designed based on the same concepts used for the smaller version. However, in order to let the device cross connect 80 channels spaced by 0.4 nm the wraparound requirements demand the WGR to operate in the diffraction order $m = 47$. Thus, N/m clearly exceeds unity so that (10) is not fulfilled any more. Therefore, we expect channels whose deviation will be larger than the distance between two adjacent output ports so that the wavelength mapping between the input and output ports is lost.

This can be seen by calculating the transmission spectra of such device. It can be shown that the channels belonging to different diffraction orders either overlap or leave gaps in between. The simulations are supported by the measurements shown in Fig. 7 where on the right side the first channel of the diffraction order $m-1$ overlaps with the last channel of the order m while on the other side of the spectrum a gap opens between the first channel of the order m and the last one of the order $m+1$.

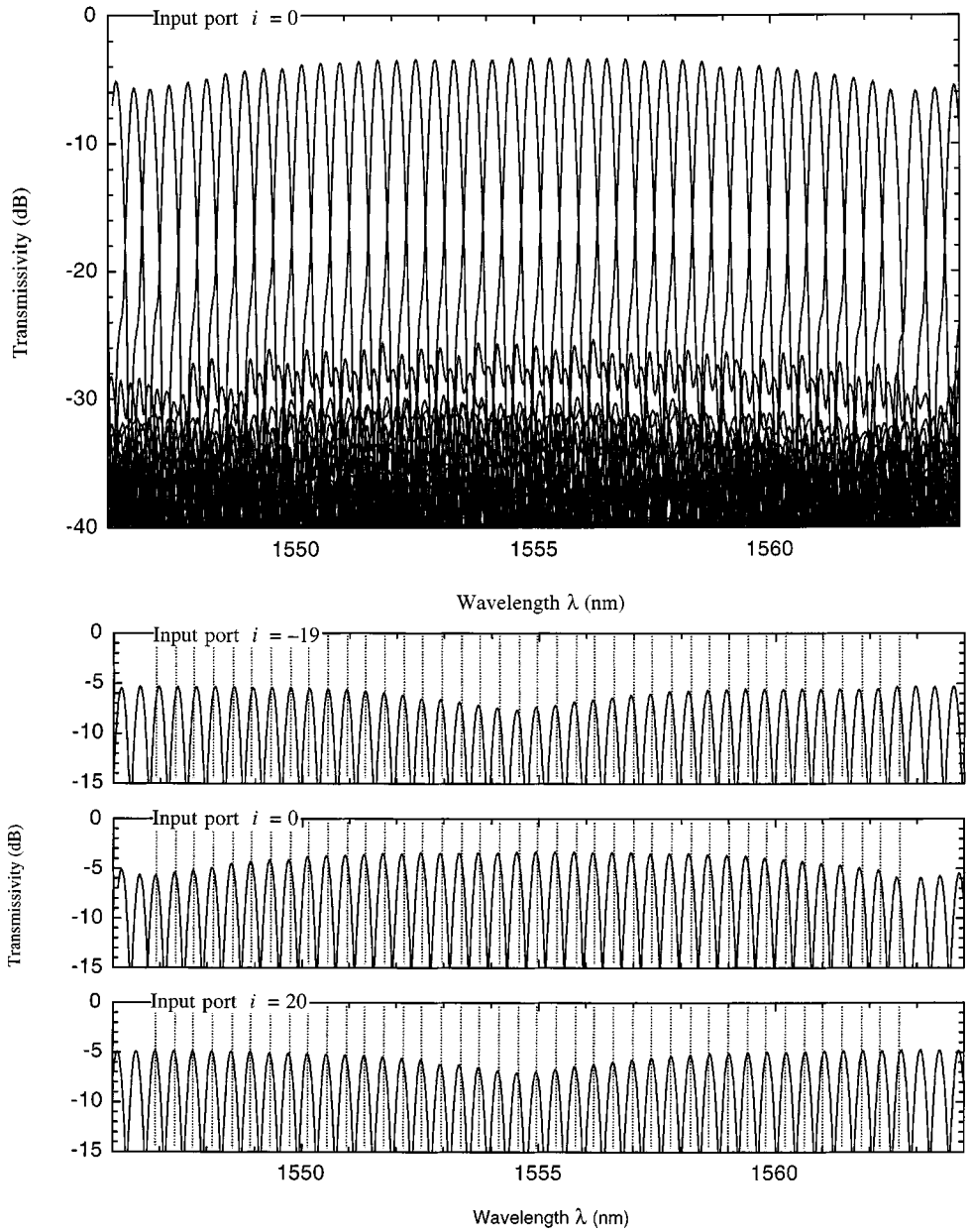

Fig. 6. (a) Measured fiber-to-fiber transmission spectra referred to the central input port ($i = 0$) in a 40×40 WGR with channels equally spaced by $\Delta\lambda = 0.4$ nm and shifted output ports. (b) Comparison among the spectra obtained from the central port (center) and the two most lateral ports (top and bottom). The dotted grid represents the channel spacing of 0.4 nm.

VII. Final Remarks

We have discussed few factors which, in a $N \times N$ WGR operating with a single set of N optical channels, can limit the maximum value of N. We have shown that an efficient operation of the WGR can be achieved for larger N when the optical channels are equally spaced in wavelength. In this case (10) gives an upper limit for N which is basically determined by the wavelength span $N\Delta\lambda$ covered by the N optical channels. Therefore, the smaller the channel spacing, the larger N. However, a lower limit to the channel spacing is set by the bit rates which the WGR has to support. In fact, if on one hand large N and thus smaller channel spacings require the device to have narrower passbands to avoid increased penalties due for example to crosstalk, on the other hand narrower passbands might introduce penalties due to the filtering effects occurring at higher bit rates. A compromise has to be found. In addition, other factors like the width of the output ports, the tolerated losses and crosstalk, can further limit N.

Experimentally, we demonstrated that by properly repositioning the output ports is still possible to access larger N although additional losses have been introduced. With this new arrangement and a given channel spacing of 0.4 nm we doubled N from 20 to 40 without affecting the worst case performance of the device. The maximum allowed by (10) is $N = 62$. We believe that a small margin for improvement is still available and 50×50 WGR might be produced.

We also realized an 80×80 WGR which, as expected, could not be operated with a single set of 80 wavelengths for all the input ports. Nevertheless, such devices can be still perfectly

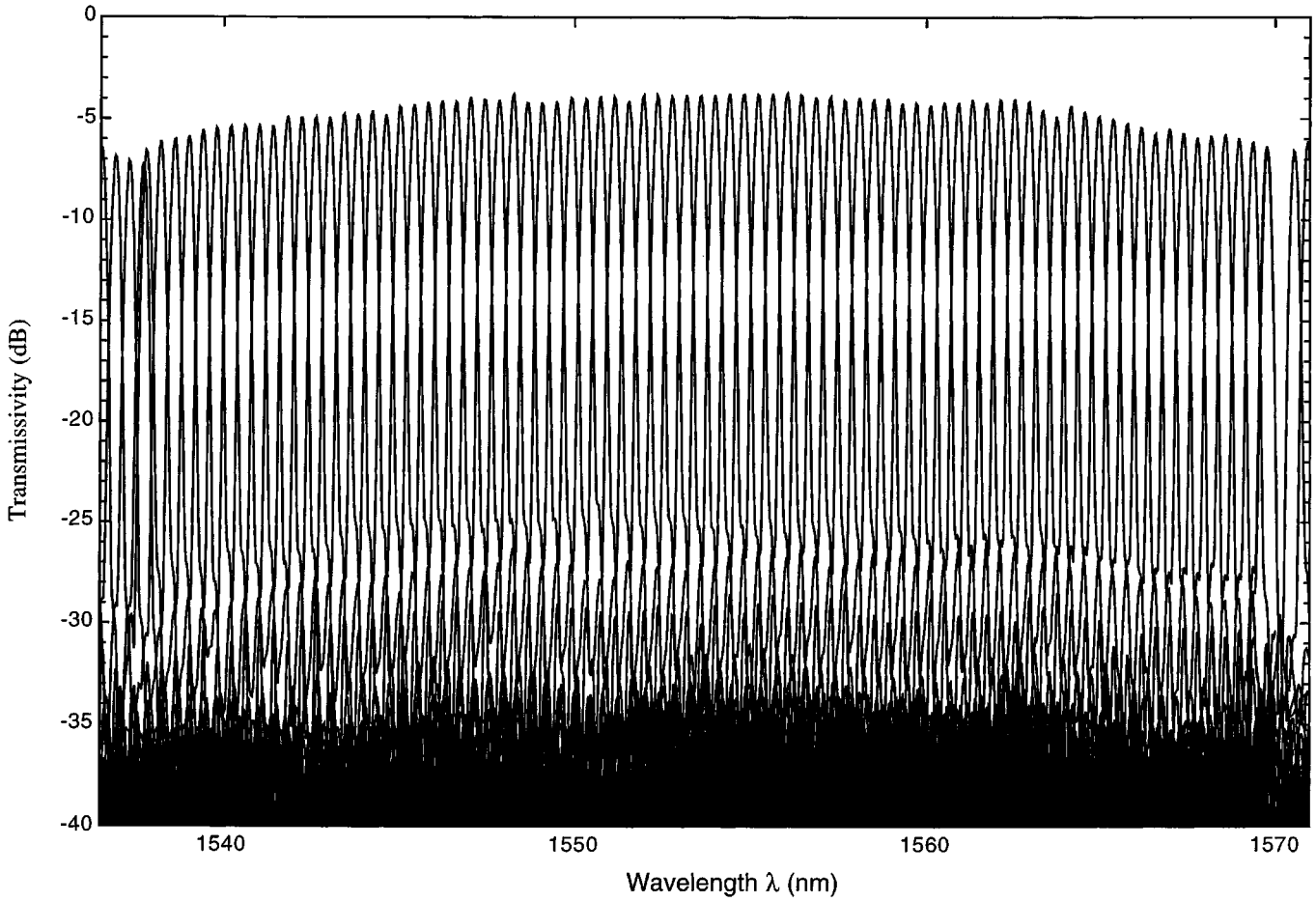

Fig. 7. Measured fiber-to-fiber transmission spectra referred to the central input port ($i = 0$) in a 80×80 WGR with channels equally spaced by $\Delta\lambda = 0.4$ nm and shifted output ports. Details in the text.

used when the system in which they are inserted allows the independent tuning of the wavelengths at each input port. It can be shown that this can be achieved when the total number of available wavelengths is $2N$.

ACKNOWLEDGMENT

The authors are indebted to M. Zirngibl, J. Fernandes, and I. Biaggio for their invaluable support.

REFERENCES

[1] C. Dragone, "An $N \times N$ optical multiplexer using a planar arrangement of two star couplers," *IEEE Photon. Technol. Lett.*, vol. 3, pp. 812–815, 1991.

[2] C. Dragone, C. A. Edwards, and R. C. Kistler, "Arrayed-waveguide grating for wavelength division multidemulti-plexer with nanometer resolution," *IEEE Photon. Technol. Lett.*, vol. 3, pp. 896–899, 1991.

[3] H. Takahashi, S. Suzuki, K. Katoh, and I. Nishi, "Arrayed-waveguide grating for wavelength division multidemulti-plexer with nanometer resolution," *Electron. Lett.*, vol. 26, pp. 87–88, 1990.

[4] K. Okamoto, K. Moriwaki, and S. Suzuki, "Fabrication of 64×64 arrayed-waveguide grating multiplexer on silicon," *Electron. Lett.*, vol. 31, pp. 184–186, 1995.

[5] K. Okamoto, T. Hasegawa, O. Ishida, A. Himeno, and Y. Ohmori, "32×32 arrayed-waveguide grating multiplexer with uniform loss and cyclic frequency characteristics," *Electron. Lett.*, vol. 33, pp. 1865–1866, 1997.

[6] H. Takahashi, K. Oda, H. Toba, and Y. Inoue, "Transmission characteristics of arrayed waveguide $N \times N$ wavelength multiplexer," *J. Lightwave Technol.*, vol. 13, pp. 447–455, 1995.

[7] M. K. Smit, "New focusing and dispersive planar component based on an optical phase array," *Electron. Lett.*, vol. 24, pp. 385–386, 1988.

P. Bernasconi, photograph and biography not available at the time of publication.

C. Doerr (M'97), photograph and biography not available at the time of publication.

C. Dragone (SM'84–F'91), photograph and biography not available at the time of publication.

M. Cappuzzo, photograph and biography not available at the time of publication.

E. Laskowski, photograph and biography not available at the time of publication.

A. Paunescu, photograph and biography not available at the time of publication.